

Sol-gel derived nanostructured cerium oxide film for glucose sensor

Anees A. Ansari,^{a)} Pratima R. Solanki, and B. D. Malhotra^{b)}

*Biomolecular Electronics and Conducting Polymer Research Group, National Physical Laboratory,
Dr. K. S. Krishnan Marg, New Delhi-110012, India*

(Received 9 April 2008; accepted 5 June 2008; published online 1 July 2008)

Sol-gel derived nanostructured cerium oxide (CeO_2) film deposited on gold (Au) electrode has been utilized for physisorption of glucose oxidase (GOx). X-ray diffraction, atomic force microscopy, UV-visible spectroscopy, and electrochemical techniques have been used to characterize sol-gel derived CeO_2/Au electrode and GOx/ CeO_2/Au bioelectrode. The response characteristics of the glucose bioelectrode (GOx/ CeO_2/Au) indicate linearity, detection limit and shelf-life as 50–400 mg/dL, 12.0 μM , and 12 weeks, respectively. The value of apparent Michaelis–Menten constant (K_m) of GOx/ CeO_2/Au bioelectrode has been found to be 13.55 μM . © 2008 American Institute of Physics. [DOI: 10.1063/1.2953686]

There is a growing interest in the development of a mediator-free biosensor to achieve direct electron transfer in metalloproteins for mimicking catalytic roles in living systems.^{1,2} Glucose biosensor is increasingly being studied because of its importance to monitor blood glucose for treatment of both diabetics and nondiabetics.^{2–4} Conducting polymers,⁵ nanomaterials,^{6–10} sol-gels,^{2,11–15} etc. have been proposed for the immobilization of glucose oxidase. Sol-gel films, due to their various characteristics such as better thermal stability, low cost, biocompatibility, non-toxicity and low temperature processing, etc. have attracted much interest.^{1,11–16} Many metal oxides such as zinc oxide,^{4,10} tin oxide,¹¹ titanium oxide,^{2,8} and zirconium oxide¹⁴ have been utilized for preparation of sol-gel films for immobilization of desired proteins.

CeO_2 has been reported to exhibit interesting properties such as electrical conductivity, large surface area, chemical inertness, nontoxicity, negligible swelling, and biocompatibility that can be used to fabricate electrochemical biosensor.^{17,18} Moreover, CeO_2 is known to have a wide band gap (3.4 eV) with high isoelectric point (IEP, 9.0) and good retention of biological activity for protein binding.¹⁷ The high IEP of sol-gel nanostructured CeO_2 can be advantageous for immobilization of low IEP enzyme (IEP of GOx, 4.2) via electrostatic interactions.

We report a glucose biosensor based on GOx immobilized nanostructured sol-gel derived CeO_2 film deposited on gold electrode. This GOx/ CeO_2/Au bioelectrode shows high affinity for glucose with enhanced sensitivity without using any electron mediator.

Nanostructured CeO_2 films have been deposited by sol-gel dip coating technique on Au coated 7059 corning glass plate. CeO_2 sol prepared using a method described in literature has been used for the fabrication of desired films.¹⁹ Au electrode ($1 \times 3 \text{ cm}^2$) is used for film deposition by dip coating technique with a selected pulling speed. The thickness of CeO_2 film is controlled by lifting speed (10 cm/min). These CeO_2 films are dried in air at room temperature and are then heat treated to 300 °C for about 3 h. The thickness of deposited film is 45 nm at room temperature estimated by atomic

force microscopy (AFM). A 5 μL GOx ($\sim 60 \text{ U/mg}$) solution is physisorbed onto CeO_2/Au electrode surface. The CeO_2/Au electrodes containing 1.0 mg/ml GOx solution in phosphate buffer saline (PBS) (50 mM, pH 7.0) kept overnight are washed with PBS and then dried at 25 °C. These GOx/ CeO_2/Au bioelectrodes are stored at 4 °C when not in use and electrochemical studies are performed at 25 °C.

X-ray diffraction (XRD) (Rigaku) studies have been done to identify the crystal structure of CeO_2 film. AFM (Veeco DCP2) studies have been conducted to examine the surface morphology. The enzyme activity and absorption spectra of CeO_2 film have been recorded using UV-visible spectrophotometer (Model 160A, Shimadzu) to investigate binding of GOx onto CeO_2/Au electrode. Electrochemical measurements have been conducted on an autolab potentiostat/galvanostat (Eco Chemie, Netherlands) using a three-electrodes cell containing Ag/AgCl as reference electrode and platinum as counter electrode in PBS containing $\text{Fe}[(\text{CN})_6]^{3-/4-}$.

Figure 1 shows results of XRD studies of sol-gel derived nanostructured CeO_2 film deposited on glass substrate. XRD pattern of CeO_2 film shows only (111) reflection at 29.36° indicating growth of oriented crystallites with axis normal to

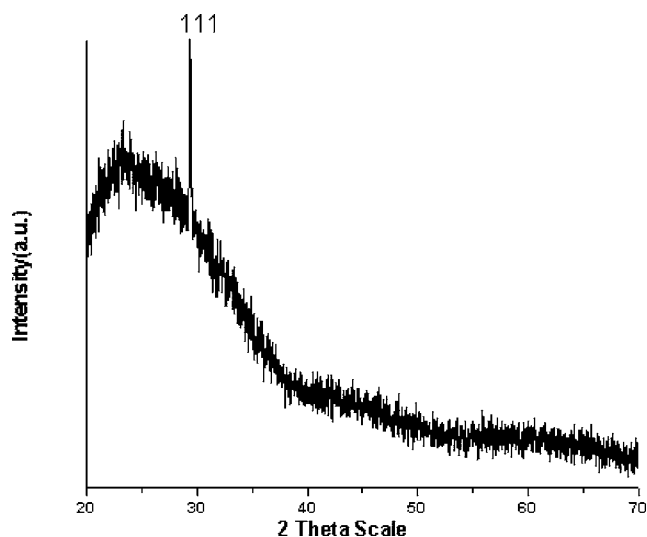


FIG. 1. XRD pattern of sol-gel derived nanostructured CeO_2 film.

^{a)}Electronic mail: aneesaansari@gmail.com.

^{b)}Electronic mail: bansi.malhotra@gmail.com. Tel.: 91-11-45609152. FAX: 91-11-45609310.

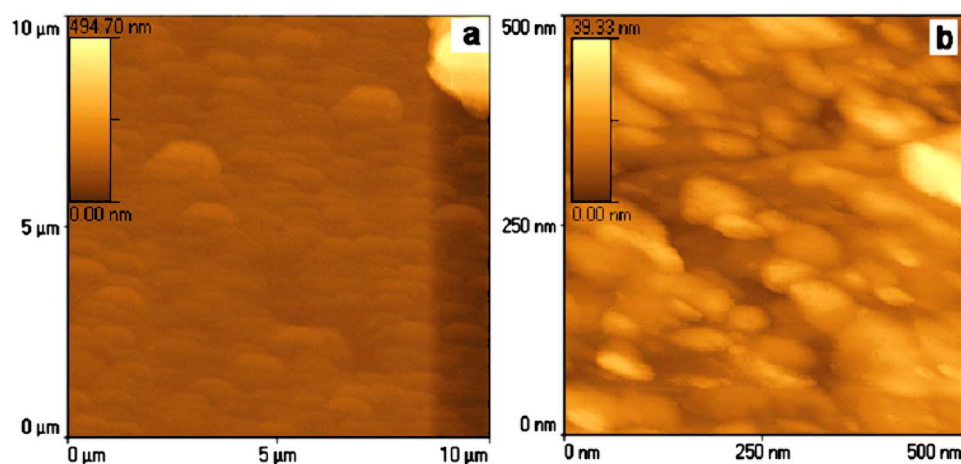


FIG. 2. (Color online) AFM of (a) sol-gel CeO₂ film (1 × 1 μm) and (b) GOx/CeO₂/Au film (3 × 3 μm).

substrate. No other crystalline forms such as Ce³⁺ or cerium compound are seen. The particle size of this film is estimated as 3 nm using Scherer equation. Compared to bulk CeO₂ (0.5411 Å), the value of lattice constant (a) of CeO₂ film calculated from the peak position as (a)=0.544 Å is slightly higher and is ascribed to elongated unit cell along the growth direction. The increased lattice constant indicates lattice expansion effect resulting from increased oxygen vacancies and Ce³⁺ ions with decreased particle size.²⁰

The AFM (Fig. 2) shows surface topography of prepared CeO₂ film, revealing formation of uniformly distributed spherical nanostructure. The surface roughness [root mean square (RMS)] of CeO₂ sol-gel film is determined to be 52 nm indicating high porosity and decreases to 5 nm after GOx immobilization and globular structure is observed at the CeO₂ surface indicating highly porous (pore size about 10 nm) surface with increased roughness. The spherical globular structure can be assigned to reduction of atmospheric oxygen in the lattice, resulting in reduction of Ce⁴⁺ to Ce³⁺ leading to generation of charge carriers.

The results of UV/visible absorption studies²¹ conducted on sol-gel derived CeO₂/Au and GOx/CeO₂/Au bioelectrode reveal absorption bands at 300 and 294 nm assigned to the charge transfer transition from O²⁻ (2p) to Ce⁴⁺ (4f) orbital in CeO₂. The observed red-shift with reduced intensity in the spectra of nanostructured GOx/CeO₂/Au bioelec-

trode is attributed to nanoparticles covalently bonded with physisorbed GOx onto CeO₂/Au electrode.²²

Differential pulse voltammetry (DPV) studies²¹ have been conducted on (a) bare Au electrode, (b) CeO₂/Au electrode, and (c) GOx/CeO₂/Au bioelectrode. The peak current decreases after CeO₂ deposition on Au electrode indicating that semiconducting CeO₂ film restricts conductive sites but allows electrochemistry to occur at the electrode. On physisorption of GOx onto CeO₂/Au electrode, magnitude of DPV peak current decreases with peak shift due to presence of insulating GOx, and low electrical conductivity of CeO₂/Au electrode results in the blocking of some conductive sites of the modified electrode.

The results of cyclic voltammetry studies [Fig. 3(a)] reveal a redox couple of ferrocyanide/ferricyanide for (a) bare Au electrode, (b) CeO₂/Au electrode, and (c) GOx/CeO₂/Au bioelectrode conducted in PBS buffer (50 mM, pH 7.0) in the range of 0.6–0.9 V. The peak potential of ferrocyanide/ferricyanide decreases and peak-to-peak separation (ΔE_p) increases in the order: bare Au electrode < CeO₂/Au electrode < GOx/CeO₂/Au bioelectrode. The peak current of CeO₂/Au electrode (curve b, Fig. 3(a)) is less than that of the bare Au electrode [curve a, Fig. 3(a)] due to deposition of sol-gel derived insulating CeO₂ layer on the electrode surface that functions as a barrier to the interfacial electron transfer. The peak current of GOx/CeO₂/Au bio-

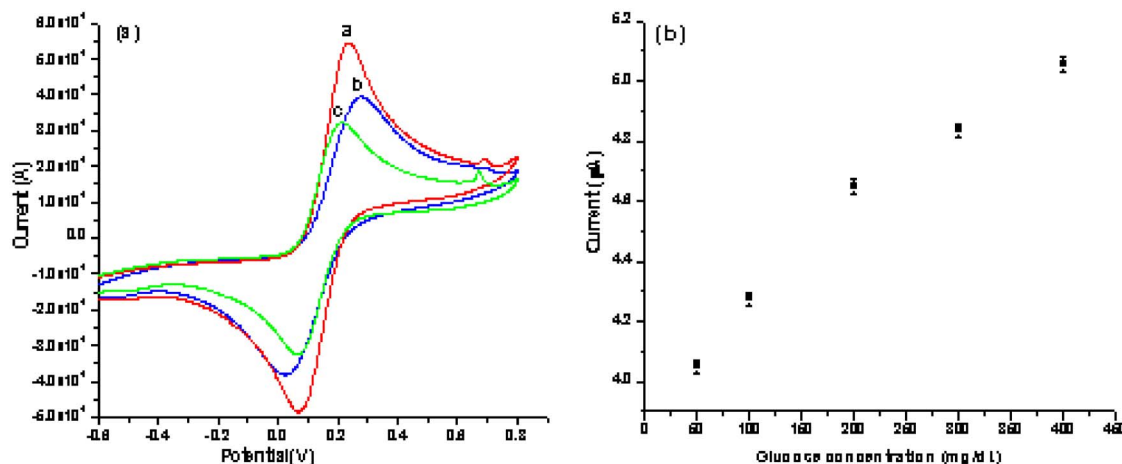


FIG. 3. (Color online) Cyclic voltammograms of (a) curve a; bare Au electrode, curve b; CeO₂/Au electrode, curve c; GOx/CeO₂/Au bioelectrode. (b) Amperometric response of GOx/CeO₂/Au bioelectrode as a function of glucose concentration.

electrode [curve c, Fig 3(a)] is much less than that of CeO₂/Au electrode. The decreased peak current could be attributed to electrostatic repulsion between oxidized GOx physisorbed on CeO₂/Au electrode and the anionic redox couple [Fe(CN)₆]^{3-/4-} ions that are negatively charged. In addition, oxidation and reduction potentials are negative and observed positive peak shift after GOx immobilization is attributed to low electrical conductivity of CeO₂ deposited electrode.

Figure 3(b) shows amperometric response of the nanostructured CeO₂/Au glucose biosensor on successive additions of glucose. The amperometric current [Fig. 3(b)] of the fabricated biosensor increases linearly (50–400 mg/dL) with increasing glucose concentration with correlation coefficient (*R*) as 0.987 indicating good electrocatalytic behavior of GOx/CeO₂/Au bioelectrode. Compared to similar glucose biosensors,^{8–10} this sensor shows higher sensitivity (0.00287 μA/mg dL⁻¹ cm⁻²) and low detection limit (12.0 μM).

The value of Michaelis–Menten constant (*K_m*) determined from Lineweaver–Burke plot as 13.55 μM is much lower than the value reported with other matrices.^{8,9} The high GOx affinity to glucose is assigned to biocompatibility, large surface area, and high electron communication capability of CeO₂ nanoparticles in nanostructured GOx/CeO₂/Au electrode surface. This glucose sensor reaches more than 95% steady state current in less than 5 s indicating faster electron communication between GOx and nanostructured CeO₂ electrode. The GOx activity measurements conducted as a function of *pH*, indicate that GOx/CeO₂/Au electrode yields maximum enzymatic activity in *pH* 7–7.5. The effect of interferents such as ascorbic acid, uric acid, urea, and cholesterol on amperometric response shows negligible effect.

The characteristics of the GOx/CeO₂/Au biosensor along with those reported in literature^{21,22} reveal that sol-gel derived nanostructured CeO₂ is a promising matrix for immobilization of GOx.

We have fabricated a cost-effective biosensor by immobilizing GOx on sol-gel derived nanostructured CeO₂ film without any additional promoter or mediator. The spectroscopic and electrochemical measurements show that sol-gel derived CeO₂ film/electrode is an excellent matrix for immobilization of GOx on CeO₂/ITO electrode surface. This nanostructured GOx/CeO₂/Au bioelectrode exhibits high sensitivity (0.002 87 μA mgdL⁻¹ cm²), linearity in the range

50–400 mg/dL, high detection limit (12.0 μM), and stability of 12 weeks. Efforts should be made to utilize the sol gel derived cerium oxide film for other biosensing applications.

We thank Dr. Vikram Kumar, Director, NPL (India) for the facilities. A.A.A. and P.R.S. thank DBT and CSIR (India) for financial support.

- ¹J. Wang, Chem. Rev. (Washington, D.C.) **108**, 814 (2007).
- ²J. Yu and H. Ju, Anal. Chem. **74**, 3579 (2002).
- ³H. Lee, S. W. Yoon, E. J. Kim, and J. Park, Nano Lett. **7**, 778 (2007).
- ⁴A. Wei, X. W. Sun, J. X. Wang, Y. Lei, X. P. Cai, C. M. Li, Z. L. Dong, and W. Huang, Appl. Phys. Lett. **89**, 123902 (2006).
- ⁵Z. Matharu, G. Sumana, S. K. Arya, S. P. Singh, V. Gupta, and B. D. Malhotra, Langmuir **23**, 13188 (2007).
- ⁶P. Pandey, S. P. Singh, S. K. Arya, V. Gupta, M. Dutta, S. Singh, and B. D. Malhotra, Langmuir **23**, 3333 (2007).
- ⁷S. Zhang, N. Wang, Y. Niu, and C. Sun, Sens. Actuators B **109**, 367 (2005).
- ⁸Q. Li, G. Luo, J. Feng, Q. Zhou, L. Zhang, and Y. Zhu, Electroanalysis **13**, 413 (2001).
- ⁹A. Salimi, E. Sharifi, A. Noorbakhsh, and S. Soltanian, Biosens. Bioelectron. **22**, 3146 (2007).
- ¹⁰J. X. Wang, X. W. Sun, A. Wei, Y. Lei, X. P. Cai, C. M. Li, and Z. L. Dong, Appl. Phys. Lett. **88**, 233106 (2006).
- ¹¹N. Q. Jia, Q. Zhou, L. Liu, M. M. Yan, and Z. Y. Jiang, J. Electroanal. Chem. **580**, 213 (2005).
- ¹²Y. Zou, C. Xiang, L. X. Sun, and F. Xu, Biosens. Bioelectron. **23**, 101 (2008).
- ¹³U. Narang, P. N. Prasad, F. V. Bright, K. Ramanathan, N. D. Kumar, B. D. Malhotra, M. N. Kamalasanan, and S. Chandra, Anal. Chem. **66**, 3139 (1994).
- ¹⁴H. J. Kim, S. H. Yoon, H. N. Choi, Y. K. Lyu, and W. Y. Lee, Bull. Korean Chem. Soc. **27**, 65 (2006).
- ¹⁵W. Z. Jia, K. Wang, Z. J. Zhu, H. T. Song, and X. H. Xia, Langmuir **23**, 11896 (2007).
- ¹⁶H. Elzanowska, E. A. Irhayem, B. Skrzynecka, and V. I. Birss, Electroanalysis **16**, 478 (2004).
- ¹⁷K.-J. Feng, Y.-H. Yang, Z.-J. Wang, J.-H. Jiang, G.-L. Shen, and R.-Q. Yu, Talanta **70**, 561 (2006).
- ¹⁸R. W. Tarnuzzer, J. Colon, S. Patil, and S. Seal, Nano Lett. **5**, 2573 (2005); Y. Y. Tsai, J. O. Cossio, K. Agering, N. E. Simpson, M. A. Atkinson, C. H. Wasserfall, I. Constantinidis, and W. Sigmund, Nanomedicine **2**, 325 (2007).
- ¹⁹T. Suzuki, I. Kosacki, and H. U. Anderson, Solid State Ionics **151**, 111 (2002).
- ²⁰S. Deshpande, S. Patil, S. Kuchibhatla, and S. Seal, Appl. Phys. Lett. **87**, 133113 (2005).
- ²¹See EPAPS Document No. E-APPLAB-93-017827 for results of UV-Visible, DPV studies and Table I. For more information on EPAPS see <http://www.aip.org/pubservs/epaps.html>.
- ²²Y. Yang, H. Yang, M. Yang, Y. Liu, G. Shen, and R. Yu, Anal. Chim. Acta **525**, 213 (2004).